

MODELLING MEDITERRANEAN FOREST PRODUCTIVITY USING ENVISAT MERIS DATA SET

Suha Berberoglu

Cenk Dönmez

Department of Landscape Architecture

University of Cukurova, Adana 01330

Turkey

suha@mail.cu.edu.tr

ABSTRACT

The aim of this study is to derive land cover products of Envisat MERIS with a 300-m pixel representation of pine forest Net Primary Productivity (NPP) of Taurus Mountain chain at the Eastern Mediterranean coast of Turkey.

The CASA model was utilised to predict annual regional fluxes in terrestrial net primary production at variable degrees of C, depending on the monthly conditions, with terrestrial net production. Calculation of annual terrestrial NPP is based on the concept of light-use efficiency, modified by temperature, rainfall values and solar radiation scalars. In addition, percentage of tree cover, land cover map of the region, soil texture and NDVI (normalized difference vegetation index) were used to constitute this model. The approach is for estimating percent tree cover employing continuous training data over the whole range of tree cover. The training data set is derived by aggregating high-resolution tree cover using IKONOS imagery to coarse scales Landsat ETM and is used with multi-temporal metrics based on 47 Envisat MERIS images recorded between March 2003 and September 2005. A regression tree algorithm is used to predict the dependent variable of tree cover based on signatures from the multitemporal metrics.

Majority of the work in the literature have been focused on global scale, however while the recent large area studies have demonstrated qualitative correspondence of relationship between ecosystem change and ecosystem function, little is known about the impacts of extrapolating quantitative relationships derived at restricted sites to very large geographic areas. This study showed that Envisat MERIS data yield greater spatial detail in the characterization of NPP at the regional scale in the Mediterranean.

INTRODUCTION

Vegetation plays an important role in the energy, matter and momentum exchange between land surface and atmosphere. Through the process of photosynthesis, land plants assimilate carbon in atmosphere and incorporate into dry matter while part of carbon is emitted into atmosphere again through plant respiration. The remainder of photosynthesis and respiration is called net primary productivity (NPP), which is important in the global carbon budget. NPP is an important component of the carbon cycle and a key indicator of ecosystem performance (Lobell *et al.* 2002). Improved methodologies for carbon source and sink accounting in agriculture and forestry will be an important input for the decision support element. Forest ecosystems are important as major terrestrial carbon reservoirs in the global carbon cycle (Dixon *et al.* 1994), it is particularly important for maintaining regional biodiversity, and hydrological integrity of catchments. Majority of the work in the literature have been focused on global scale, however while the recent large area studies have demonstrated qualitative correspondence of relationship between ecosystem change and ecosystem function, little is known about the impacts of extrapolating quantitative relationships derived at restricted sites to very large geographic areas. There is abundant experimental evidence supporting these assumptions in particular for Mediterranean region where will severely be affected by climate change. NPP has been mapped on a global scale using NDVI images accompanied by models which calculate NPP as a function of the driving energy for photosynthesis, the absorbed photosynthetically active (400 to 700 nm) solar radiation (APAR), and an average light utilization efficiency (ϵ) (Potter *et al.* 1993, Ruimy *et al.* 1994, Prince and Goward 1995, Malmstrom *et al.* 1997). Running *et al.* (1999) suggested the variation of three factors deserve further study in the context of using remote sensing to derive spatial estimates of NPP: 1) spatial resolution 2) land cover and 3) light use efficiency (LUE) estimates.

In previous studies, large area NPP has been predicted at spatial resolutions of 1 km using Advanced Very High Resolution Radiometer (AVHRR) data (Goetz *et al.* 1999) and of 500 m using Moderate Resolution Imaging Spectrometer (MODIS) data. Considering the wide range of approaches to modeling NPP, it is evident that the choices of grain size and model structure, although often selected for practical reasons, may seriously affect the accuracy of modeled NPP data. Multiple land cover types often exist even within a 1 km cell, and can have variable leaf area index (LAI), canopy chemistries, phenology, leaf structure, and production efficiencies.

Envisat MERIS is a potentially valuable sensor for the measurement and monitoring of terrestrial environments at regional to global scales (Verstraete *et al.*, 1999). Envisat MERIS is one of the payloads on the European Space Agency's Envisat and is radiometrically the most accurate imaging spectrometer in space (Dash and Curran 2004). It has 15 programmable (2.5–20 nm wide) wavebands in the 390–1040 nm region and a spatial resolution of 300 m. In the standard band setting, it has five discontinuous wavebands in red and near-infrared (NIR) wavelengths with band centres at 665 nm, 681.25 nm, 708.75 nm, 753.75 nm and 760.625 nm (Dash and Curran 2004). So, the primary theme of this paper is to generate a production efficiency model which can be derived land cover products of Envisat MERIS data set with a medium resolution (300 m) representation of pine forest NPP of Taurus Mountain chain at the Eastern Mediterranean coast of Turkey using the Carnegie-Ames-Stanford approach (CASA) (Potter *et al.* 1993).

STUDY AREA AND DATA

The study area is located on the Taurus Mountain chain in the Eastern Mediterranean region of Turkey (Figure 1).



Figure 1. The location of the study area.

The region covers an area of approximately 21.45 km² and comprises pure and mixed conifer forests. These forests are classified as a Mediterranean evergreen cover type (Koppen, 1931) and estimated to be approximately 100 years old from tree cores. Dominant tree species are Crimean pine (*Pinus nigra*), Lebanese cedar (*Cedrus libani*), Taurus fir (*Abies cilicica*), Turkish pine (*Pinus brutia*), and juniper (*Juniperus excelsa*) (Davis, 1965). The prevailing climate is Mediterranean characterized by mild and rainy winters and hot and dry summers. The total annual rainfall is approximately 800 mm. Rainfall is variable in amount and timing in that 75% of rain falls mainly during autumn and winter. The mean annual temperature between 1990 and 2002 was 19 C, with mean minimum and maximum temperatures of 8 C in January and 30 C in July, respectively (TSMS, 2005). Dominant soils of the forest stands are classified as Lithic Xerorthent of Entisol and developed on fluvial and lacustrine materials during the Oligocene Epoch (Soil Survey Staff, 1998).

An Envisat MERIS data set comprising 47 images from March 2003 to September 2005 was selected (Figure 2). Three sub-scenes of multi-spectral IKONOS imagery representing different types of forest cover recorded in May 2002 were used as training and testing data for percent tree estimation. Other data utilised in the analysis included 1:25,000 scale Government Forestry Department and topographic maps and aerial photographs.

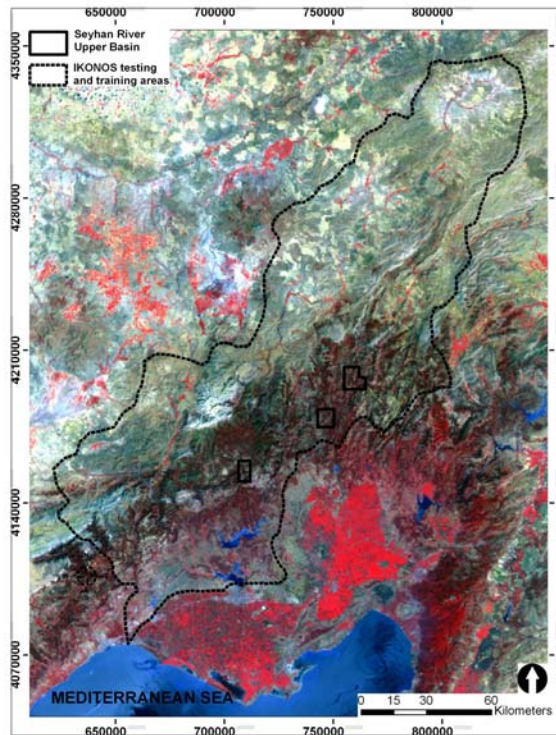


Figure 2. Envisat MERIS image showing study area and the IKONOS training and testing areas.

MODELLING AND MAPPING NPP

Land and ocean models, calculates NPP as a function of the driving energy for photosynthesis, the absorbed photosynthetically active (400 to 700 nm) solar radiation (APAR), and an average light utilization efficiency (ϵ).

$$\text{NPP} = \text{APAR} \times \epsilon$$

The monthly NPP flux, defined as net fixation of CO₂ by vegetation, is computed in CASA on the basis of light-use efficiency (Monteith, 1972). The fundamental relation in the CASA model is

$$\text{NPP} = f(\text{NDVI}) \times \text{PAR} \times \epsilon \times g(T) \times h(W)$$

where APAR (in megajoules per square meter per month) is a function of NDVI and downwelling photosynthetically active solar radiation (PAR) and ϵ (in grams of C per megajoule) is a function of the maximum achievable light utilization efficiency ϵ adjusted by functions that account for effects of temperature $g(T)$ and water $h(W)$ stress (Potter *et al.* 1993). Whereas previous versions of the CASA model (Potter *et al.* 1993, 1999) used a normalized difference vegetation index (NDVI) to estimate FPAR, the current model version instead relies upon canopy radiative transfer algorithms (Knyazikhin *et al.* 1998), which are designed to generate improved FPAR products as inputs to carbon flux calculations. The model was utilized to predict annual regional fluxes in terrestrial net primary production at variable degrees of C, depending on the yearly conditions, with terrestrial net production. Several diverse datasets were used in this research. Calculation of annual terrestrial NPP is based on the concept of light-use efficiency, modified by temperature, rainfall values and solar radiation scalars. In addition, percentage of tree cover, land cover map of the region, soil texture and NDVI (normalized difference vegetation index) will be used to constitute this model.

Climate Data

The climate data includes monthly precipitation, air temperature, solar radiation scalars. These datasets are generated based on 9 years (1994-2003) records from 50 climate stations in Seyhan Watershed. Geostatistical spatial interpolation which means cokriging method was implemented together with digital elevation data to map climate variables on a monthly basis. The output was 300 m spatial resolution and accuracy was tested by absolute difference analysis with comparison to original station values.

Estimation of Percent Tree Cover

In the past decade, several efforts to estimate tree canopy cover as a continuous variable have been made by utilizing multiple linear regression (MLR) (Zhu and Evans 1994; DeFries *et al.*, 2000), linear mixture modelling (LMM) (Iverson *et al.* 1989), and regression tree (RT) (e.g., Hansen *et al.*, 2000; Hansen *et al.* 2003; Hansen *et al.* 2005). Among these techniques, the regression tree technique is well suited for percentage tree cover mapping because, as a non-parametric classifier, it requires no prior assumptions about the distribution of the training data. This section provides a general description of the regression tree.

The methodology for this study consisted of five steps:

- i) generate reference percentage tree cover data,
- ii) derive metrics from Envisat MERIS data,
- iii) select predictor variables,
- iv) fit RT models
- v) undertake accuracy assessment and
- vi) produce final model and map (Figure 3)

i) Modelling percent tree cover relies on the quality of training and testing data. Digital multispectral IKONOS images with a spatial resolution of 4 m were used to derive reference percentage tree cover data needed to train the model. Three sub-scenes of IKONOS images representing different forest cover types were classified and recoded to tree and non-tree pixels at a 4 m spatial resolution. This data set covered an area of 120 km². The classification results were then converted to estimate percentage tree cover at the MERIS spatial resolution. The coverage of this IKONOS data set was equal to 1232 Envisat MERIS pixels.

ii) Four vegetation biophysical variables including: normalised difference vegetation index (NDVI), leaf area index (LAI), fraction of photosynthetically active radiation (fPAR), fCover and MERIS terrestrial chlorophyll index (MTCI) were derived in addition to 15 spectral bands of Envisat MERIS data in the 390 nm to 1040 nm spectral range. LAI, fPAR and fCOVER were derived using the Top of canopy Land Products (TOA_VEG version 3) algorithm developed by Weiss *et al.* (2006).

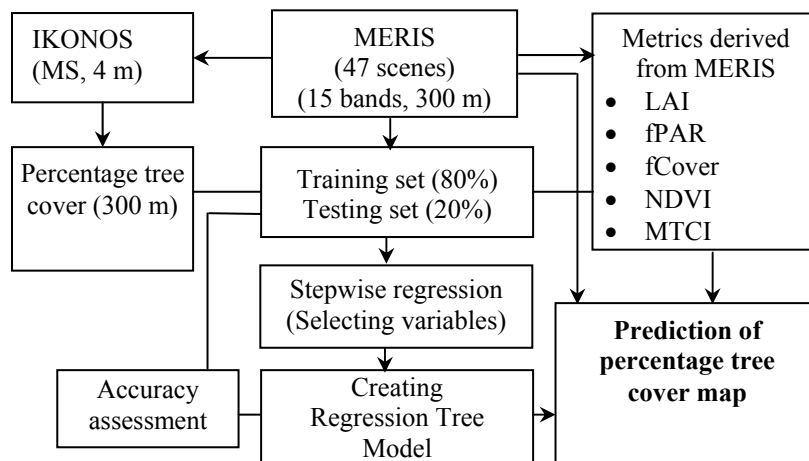


Figure 3. Summary of percentage tree estimates using regression tree method.

This was implemented using the "Visualisation and Analyzing Tool" of the MERIS/(A)ATSR Toolbox (VISAT) (Weiss *et al.*, 2006). A new index called MTCI developed by Dash and Curran (2004) is a ratio of the

difference in reflectance between band 10 and band 9 and the difference in reflectance between band 9 and band 8 of the Envisat MERIS standard band setting.

$$\begin{aligned} \text{MTCI} &= \frac{R_{\text{Band10}} - R_{\text{Band9}}}{R_{\text{Band9}} + R_{\text{Band8}}} \\ &= \frac{R_{753.75} - R_{708.75}}{R_{708.75} + R_{681.25}} \end{aligned}$$

where $R_{753.75}$, $R_{708.75}$, $R_{681.25}$ are the reflectances in the centre wavelengths of the Envisat MERIS standard band setting.

iii) Predictor variable selection involved feature selection for the most relevant input variables for the percent tree cover modelling. This was accomplished using the Stepwise Linear Regression (SLR) method from S-PLUS (Insightful Corp. 2001), which also provides classification and regression tree software. The SLR method selects the best subset of predictor variables to be employed in regression tree modelling using a stepwise procedure, which repeatedly alters the model at the previous step by adding or removing predictor variables (Helsel and Hirsch 1992). The C_p statistic is expressed as:

$$C_p = p + \frac{(n - p)(s_p^2 - \sigma^2)}{\sigma^2}$$

where n is the number of observations (number of training data), p is the number of coefficients (number of predictor variables plus one), s_p^2 is the mean square error (MSE) of the prediction model, and σ^2 is the minimum mean squared error (MSE) among the possible models (Rokhmatuloh *et al.*, 2005). The C_p statistic for each variable was examined. The C_p statistic provides a convenient criterion for determining whether a model is more accurate by adding or removing the predictor variables. The C_p statistic specifies which predictor variables are significantly related to percentage tree cover prediction.

iv) The IKONOS data set was split into two subsets; training (1023 pixels) and testing (209 pixels). The four models were fitted using the most relevant input variables selected using the SLR method and the available training with the reference data derived from IKONOS images, relationships between tree cover density and Envisat MERIS spectral values were modeled using RT technique.

v) The accuracy of the final model was obtained through validation using testing data. Model performance was measured using the correlation coefficient (r) between the predicted and actual tree cover values for the set aside test samples, r can be considered a measure of the precision of prediction.

vi) Final output consisted of spatially distributed estimates of percentage tree cover at 300 m spatial resolution and error estimates obtained through validation (Figure 4).

Mapping Land Cover

The study benefits from a large and detailed land cover database derived from four data sources: Landsat ETM image dated 17 August 2003, topographic maps, State Hydraulic Works (DSI) land cover records and ground data from field surveys. The Landsat ETM image was geometrically corrected and geocoded to the Universal Transverse Mercator (UTM) coordinate system by using 1:25,000 scale topographic maps.

Image classification was carried out using maximum likelihood algorithm with supervised training (Figure 5). The classifier was provided with the spectral reflectance properties of each class in the form of the mean reflectance for each spectral waveband and the associated covariance matrix. This data was generated from a selection of sample training pixels for each class provided from ground data. The output comprised 27 land cover classes with 30 m spatial resolution initially. The land cover classes were amalgamated to 7 classes as defined by CASA model. These data were then rasterized to 300 m cell size.

Soil Texture

The soil texture data file is based on FAO soil texture classification which has 7 classes. The dominant soil type in a soil unit, the designation "coarse", "medium", "fine", or a combination of these based on the relative amounts of

clay, silt, and sand present in the top 30 cm of soil. The regional soil maps in 25,000 scale was utilized for this study and soil texture classes were assigned on the basis of estimated clay content according to FAO (Potter *et al.* 1998).

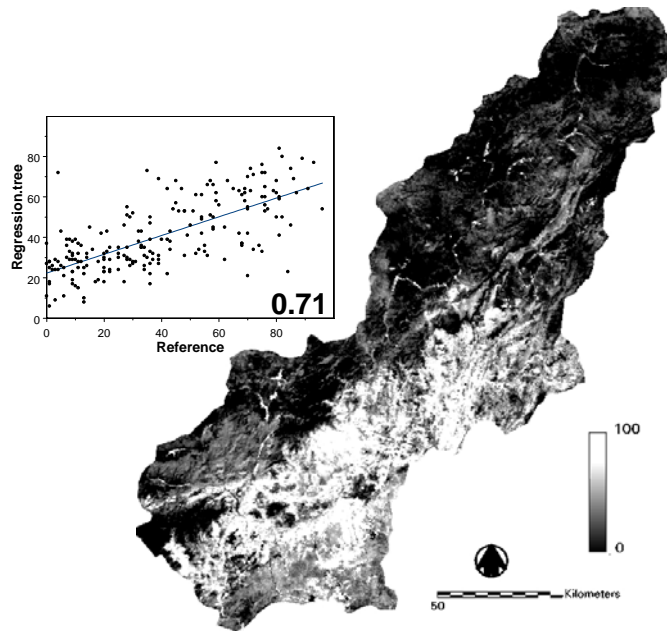


Figure 4. Percentage tree cover predictions resulting from the RT model and plot of predicted vs estimated tree cover for a sample of 209 pixels.

NDVI

Monthly NDVI images derived from 47 Envisat MERIS images recorded in between March 2003 and September 2005. The monthly composites were created and bands 10 and 6 were used to produce NDVI. Monthly NDVI images ranging between 0 and 1 were the input to CASA model.

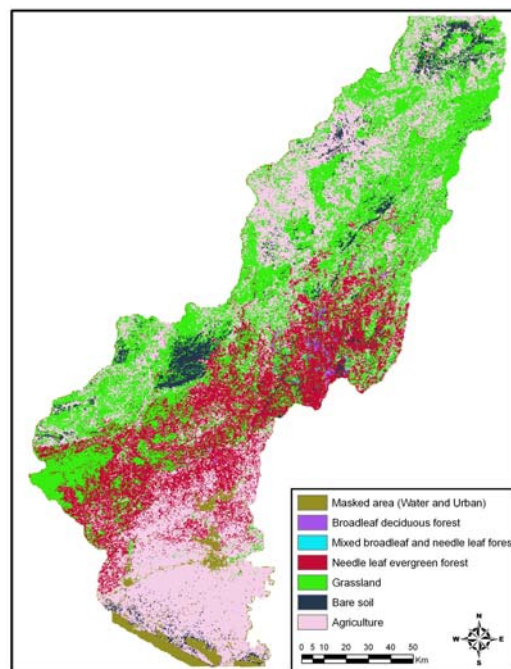


Figure 5. Land cover map derived from Landsat ETM image.

RESULTS

This study shows that Envisat MERIS data may capture the heterogeneity of Mediterranean land cover for estimating NPP. The output of the model was monthly NPP maps. The mean NPP differed significantly among all months ranged from 0.65 to 125 gC m⁻² yr⁻¹. The monthly changes of estimated NPP are shown in figure 6.

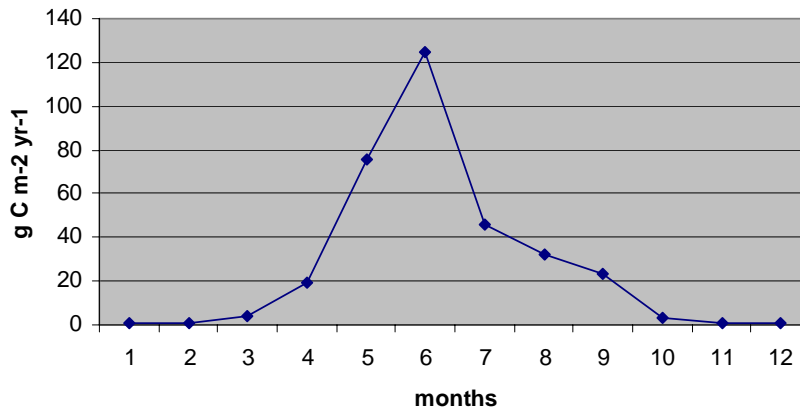


Figure 6. NASA-CASA monthly NPP results.

Both monthly and total NPP were mapped at a 300 m grid cell size (Figure 7).

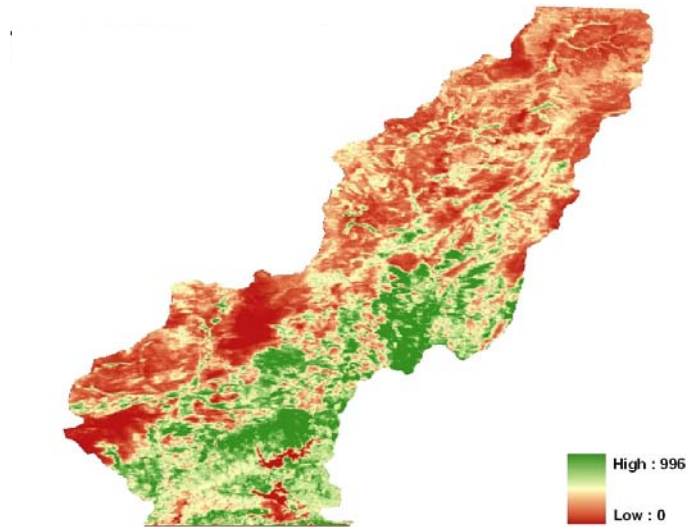


Figure 7. Predicted annual variation in NPP fluxes for Seyhan Watershed.

Spatial variation in NPP in the terrestrial components of the model is driven mostly through variation in light capture by photosynthetic biomass or APAR and secondarily through variation in ϵ (Field et al., 1995). Spatial and seasonal variation in photosynthetic biomass is, in turn, largely controlled by the availability of other resources. Consequently, regional and seasonal distributions of NPP reflect the interface between physical (e.g., precipitation, PAR,) and biological processes (e.g., species composition, microbial activity, and interactions among organisms). The estimated average NPP was approximately 388.79 gC m⁻² per year in the area (table 1).

Table 1. Annual NPP of the major units of the Seyhan Watershed, from CASA.

Classes	Mean Total NPP
Masked area (Water and Urban)	
Broadleaf deciduous forest	588.71
Mixed broadleaf and needle leaf forest	469.11
Needle leaf evergreen forest	514.22
Grassland	233.09
Bare soil	185.17
Agriculture	342.44

CONCLUSIONS

CASA model results reveal important patterns of geographic variability in NPP within a local area of Mediterranean environment. A unique advantage of combining ecosystem modeling with satellite drivers for vegetation cover properties is to enhance the spatial resolution of sink patterns for CO₂ in the terrestrial biosphere. This study reviewed the potential use of common NPP modelling technique over a Mediterranean type watershed using Envisat MERIS imagery. The main finding of this study was:

- Envisat MERIS data hold great potential for predicting NPP with CASA model because of its spatial and spectral resolutions. It can include the spatial heterogeneity of Mediterranean environment to the NPP modelling.
- CASA was the appropriate model for handling the variability present in complex and highly variable Mediterranean type forest which has sparse coverage and high species diversity. It is promising approach for modelling NPP using with Envisat MERIS imagery in this environment.
- Calcareous soil has great effect on the reflectance from a sparse Mediterranean forest cover. High reflectance from soil causes a soil albedo effect, hence soil background reflected signal overwhelms the relatively small vegetation reflected component. As a result of this, some techniques may suffer from underestimation of NPP.
- Envisat MERIS images recorded in summer months which are driest season in the Mediterranean improved overall vegetation cover discrimination. Hansen *et al.* (2002) state that some grasslands at peak greenness are indistinguishable from woodlands, and dry season imagery improves their characterization
- Regression Tree explored the complex relationships between Envisat MERIS wavebands and percent tree cover. Explanatory variables were individual Envisat MERIS wavebands, and biophysical variables such as, NDVI, LAI, fPAR and MTCI. They provided sufficient information for modelling tree cover and increased the accuracy. It also allows for the calibration of the model along the entire continuum of tree cover, avoiding the problems of using only endmembers for calibration.

REFERENCES

- Dash, J., and P. J. Curran, 2004. The MERIS terrestrial chlorophyll index, *International Journal of Remote Sensing*, 25: 5403–5413.
- Davis, P.H., 1965. Flora of Turkey and the East Aegean Islands 1(9), Edinburgh University Press, Edinburgh, UK.
- Defries, R. S., M. C. Hansen, and J. R. G. Townshend (2000). Global continuous fields of vegetation characteristics: a linear mixture model applied to multi-year 8km AVHRR data, *International Journal of Remote Sensing*, 21: 1389-1414.
- Dixon, R.K., Brown, S, Houghton, R.A, Solomon, A.M. Trexler, M.C. & Wisniewski, J. (1994). Carbon pools and flux of global forest ecosystems. *Science*, 263: 185–190.
- Field, C. B., J. T. Randerson, and C. M. Malmstrom 1995. Global net primary production: Combining ecology and remote sensing. *Remote Sensing of Environment*, 51: 74– 88.
- Goetz, S.J., D. Stephen, Prince, N. Samuel, Goward, M. Michelle, Thawley, Jennifer Small (1999). Satellite remote sensing of primary production: an improved production efficiency modeling approach. *Ecological Modelling* 122: 239–255.
- Hansen, M.C., J.R.G. Townshend, R.S. Defries, and M. Carroll (2005). Estimation of tree cover using MODIS data at global, continental and regional/local scales, *International Journal of Remote Sensing*, 26: 4359–4380.

- Hansen, M.C., R.S. Defries, J.R.G. Townshend, and R.A. Sohlberg (2000). Global land cover classification at 1km spatial resolution using a classification tree approach, *International Journal of Remote Sensing*, 21: 1331–1364.
- Hansen, M.C., R.S. Defries, J.R.G. Townshend, M. Carroll, C. Dimiceli, and R.A. Sohlberg (2003). Global percent tree cover at a spatial resolution of 500 metres: First results of the MODIS vegetation continuous fields algorithm. *Earth Interactions*, 7, paper no. 10. <http://earthinteraction.org>.
- Hansen, M.C., R.S. Defries, J.R.G. Townshend, M. Carroll, C. Dimiceli, and R.A. Sohlberg (2003). Global percent tree cover at a spatial resolution of 500 metres: First results of the MODIS vegetation continuous fields algorithm. *Earth Interactions*, 7, paper no. 10. <http://earthinteraction.org>.
- Hansen, M.C., R.S. Defries, J.R.G. Townshend, R.A. Sohlberg, C. Dimiceli, and M. Carroll (2002). Towards an operational MODIS continuous field of percent tree cover algorithm: Examples using AVHRR and MODIS data, *Remote Sensing of Environment*, 83: 303–319.
- Helsel, D.R., and R.M. Hirsch (1992). *Statistical Methods in Water Resources*, Elsevier Science Publishers B.V, Amsterdam, The Netherlands.
- Insightful Corp (2001). *S-Plus 6.2. Guide to Statistics*, Volume 2. Seattle, Washington.
- Iverson, L.R., E.A. Cook, and R.L. Graham (1989). A technique for extrapolating and validating forest cover across large regions: calibrating AVHRR data with TM data, *International Journal of Remote Sensing*, 10: 1805–1812.
- Knyazikhin, Y., J.V. Martonchik, R.B. Myneni, D.J. Diner, S.W. Running (1998). Synergistic algorithm for estimating vegetation canopy leaf area index and fraction of absorbed photosynthetically active radiation from MODIS and MISR data. *Journal of Geophysical Research* 103: 32257– 32276.
- Koppen, W., 1931. *Grundriss der Klimakunde*, Walter de Gruyter & Co.
- Lobell, D.B., J.A. Hicke, G. P. Asner, C.B. Field, C. J. Tucker, S.O. Los (2002). Satellite estimates of productivity and light use efficiency in nited States agriculture 1982–1998. *Glob. Chem. Biol.* 8: 722–735.
- Los, S. O., G. J. Collatz, P. J. Sellers, C. M. Malmstrom, N. H. Pollack, R. S. DeFries, L. Bounoua, M. T. Parris, C. J. Tucker, and D. A. Dazlich (2000). A global 9-yr biophysical land surface dataset from NOAA AVHRR data, *J. Hydrometeorol.*, 1, 183– 199, Estimation of tree cover using MODIS data at global, continental and regional/local scales.
- Malmstro, M., C. M. Thompson, M.V. Juday, G. P. Los, S. O, J. T. Randerson, and C.B. Field (1997). Interannual variation in global-scale net primary production: testing model estimates. *Global Biogeochemical Cycles*, 11: 367–392.
- Monteith, J.L (1972). Solar radiation and productivity in tropical ecosystems. *Journal of Applied Ecology* 9: 747–766.
- Potter C.S., A. Davidson, S. Klooster, D. Nepstad, H. Gustavo, H. Denegreiros, V. Brooks (1998). Regional Application of an Ecosystem Production Model for Studies of Biogeochemistry in Brazilian Amazonia, *Global Change Biology* pp. 315-333.
- Potter, C.S., J.T. Randerson., C.B Field, P.A. Matson, P.M. Vitousek, H.A. Mooney, S.A. Klooser (1993). Terrestrial ecosystem production: A process model based on global satellite and surface data. *Global Biogeochemical Cycles*, 7: 811-841.
- Prince, S. D., And Goward, S. N (1995), Global primary production: a remote sensing approach. *Journal of Biogeography*, 22: 815–835.
- Rokhmatuloh, R., H. Al-Bilbisi, K. Arihara, T. Kobayashi, D. Nitto, B. Erdene, K. Hirabayashi, T.A. Javzandulam, S.A. Lee, E. Migita, N. Soliman, Y. Ouma, M. Aslam, and R. Tateishi, (2005). Application of Regression Tree Method for Estimating Percent Tree Cover of Asia with QuickBird images as training data, The 11th CReS International Symposium on Remote Sensing, Chiba University, Chiba, Japan.
- Ruimy, A., G. Dedieu, and B. Saugier (1994). Methodology for the estimation of terrestrial net primary production from remotely sensed data, *Journal of Geophysical Research.*, 99(D3): 5263– 5284.
- Running, S. W., D. D. Baldocchi, D. P. Turner, S.T. Gower, P.S. Bakwin and K.A. Hibbard (1999). A global terrestrial monitoring network integrating tower fluxes, flask sampling, ecosystem modeling and EOS satellite data. *Remote Sensing of Environment*, 70: 108– 127.
- Soil Survey Staff, 1998. *Keys to Soil Taxonomy*, USDA-NRCS, US Government Printing Office, Washington, DC.
- Weiss, M., F. Baret, K. Pavageau, D. Béal, B. Berthelot, and P. Regner (2006). Top of canopy Land Products (TOA_VEG), Contract ESA AO/1-4233/02/I-LG.
- Zhu, Z., and D.L. Evans (1994). U.S. forest typesand predicted percent forest cover from AVHRR data, *Photogrammetric Engineering and Remote Sensing*, 60: 525–531.